

Article

## Preparation of Potassium Ferrate from Spent Steel Pickling Liquid

Yu-Ling Wei \*, Yu-Shun Wang and Chia-Hung Liu

Department of Environmental Science and Engineering, Tunghai University, Taichung 40704, Taiwan; E-Mails: sonickof2000@hotmail.com (Y.-S.W.); g02340013@thu.edu.tw (C.-H.L.)

\* Author to whom correspondence should be addressed; E-Mail: yulin@thu.edu.tw; Tel.: +886-4-2359-1368; Fax: +886-4-2359-6858.

Academic Editors: Suresh Bhargava and Rahul Ram

Received: 31 July 2015 / Accepted: 18 September 2015 / Published: 24 September 2015

---

**Abstract:** Potassium ferrate ( $K_2FeO_4$ ) is a multi-functional green reagent for water treatment with considerable combined effectiveness in oxidization, disinfection, coagulation, sterilization, adsorption, and deodorization, producing environment friendly Fe(III) end-products during the reactions. This study uses a simple method to lower Fe(VI) preparation cost by recycling iron from a spent steel pickling liquid as an iron source for preparing potassium ferrate with a wet oxidation method. The recycled iron is in powder form of ferrous (93%) and ferric chlorides (7%), as determined by X-ray Absorption Near Edge Spectrum (XANES) simulation. The synthesis method involves three steps, namely, oxidation of ferrous/ferric ions to form ferrate with NaOCl under alkaline conditions, substitution of sodium with potassium to form potassium ferrate, and continuously washing impurities with various organic solvents off the in-house ferrate. Characterization of the in-house product with various instruments, such as scanning electron microscopy (SEM), ultraviolet-visible (UV-Vis), X-ray diffraction (XRD), and X-ray absorption spectroscopy (XAS), proves that product quality and purity are comparative to a commercialized one. Methylene blue (MB) de-colorization tests with in-house potassium ferrate shows that, within 30 min, almost all MB molecules are de-colored at a Fe/carbon mole ratio of 2/1.

**Keywords:** potassium ferrate; wet oxidation method; steel pickling liquid; ferrous chloride; ferric chloride; Fe *k*-edge XAS

---

## 1. Introduction

### 1.1. Environmental Application of Potassium Ferrate

Potassium ferrate ( $K_2FeO_4$ ) is a potent oxidant. Under acidic and alkaline conditions, its respective reduction potentials are 2.20 and 0.700 V, being a potential for replacing traditional oxidants, such as ozone, hypochlorite, permanganate, and others [1]; their respective half-cell reduction potentials in acidic conditions are 2.08, 1.48, and 1.69 V, respectively [2], all less than Fe(VI). Potassium ferrate, other than acting as a powerful oxidant, can be an inorganic coagulant when chemically reduced to  $Fe(OH)_3$ ; it can effectively remove suspended solids, heavy metals, and a variety of contaminants in water [3–7]. Further, using traditional oxidants to treat pollutants/contaminants usually can result in a noteworthy toxic byproduct problem, such as tri-halo-methane and bromates [8]. In contrast, potassium ferrate, as a water treatment agent, is reduced to environment friendly  $Fe(OH)_3$  [3,9–13]. Prior to the chlorination process for drinking water, using Fe(VI) as a pre-treatment agent can effectively reduce the formation of hazardous by-products [14,15].

Despite the advantages Fe(VI) can provide, it is expensive for using it to treat pollutants and contaminants. Synthesizing Fe(VI) by using spent steel pickling liquid as an iron source can achieve a dual-win benefit by not only reducing the cost of Fe-source raw chemicals for Fe(VI) synthesis but also recycling spent steel pickling liquid for sustainable spirits. Currently, the annual output rate of spent steel pickling liquid is approximately 150,000 tons in Taiwan [16], and it is considered hazardous due to its high content of various toxic metals that may be a constraint on preparation of Fe(VI) from the pickling liquid.

### 1.2. Source of Spent Pickling Liquid

Spent pickling liquid is unwantedly produced by the steel industry. Products like steel plates, pipes, and coils always require cleaning with acid to remove their surface impurities before being subjected to further processing. The impurities include black surfaces, iron oxides, and other contaminants. Hydrochloric acid is usually used as the pickling acid for carbon steel products due to its relatively lower price, lower acid consumption rate, and providing a faster pickling process, despite its shortcomings of a larger volatilization rate [17,18].

If spent pickling liquid is treated as waste water, toxic metal present in it is generally removed through different approaches, such as precipitation method, ion exchange, and others. Among them, precipitation as hydroxide is the most often used technology. Although the technology is technically simple, its neutralization step requires a large amount of alkaline- or alkaline earth-based chemicals, and it would be much more praised if spent steel pickling liquid can be recycled.

When hydrochloric acid is used as pickling agent, most iron in spent steel pickling liquid would be present in a form of ferrous chloride through the following chemical reaction [17]:



### 1.3. Fe(VI) Preparation with Wet Oxidation Method

Oxidants used for Fe(VI) preparation in previous studies include hypochlorite, Cl<sub>2</sub>, and ozone [19]. Among them, ozone is the most powerful [19]. However, this study uses hypochlorite due to its relative ease in laboratory handling. Yet, in our further study, utilization of ozone for Fe(VI) preparation from spent pickling liquid is worthy of study. Theoretically, with the use of hypochlorite, Fe(III) can be oxidized to Na<sub>2</sub>FeO<sub>4</sub> in strong basic solution. After adding saturated KOH solution to replace the sodium of Na<sub>2</sub>FeO<sub>4</sub>, potassium ferrate precipitate can then be formed, separated, washed with organic solvents, and de-watered. Below are the associated chemical reactions [20].



Both the purity and yield of potassium ferrate is affected by the types of oxidants and iron precursors used for its preparation. In general, the use of hypochlorite (OCl<sup>-</sup>) can lead to more yield and higher purity, as compared to that using chlorine. As to iron source, ferric nitrate Fe(NO<sub>3</sub>)<sub>3</sub> · 9H<sub>2</sub>O is more expensive than ferric chloride, which can result in a more rapid synthesis rate and more yield than ferric chloride. As this study intends to recover the spent steel pickling liquid as raw material for potassium ferrate synthesis, there will be no other choice in the aspect of the identity of iron source.

One more thing that needs consideration is what kinds of organic solvents ought to be used for washing crude product potassium ferrate. Organic solvents can barely dissolve potassium ferrate, and their function is to remove the impurities, such as moisture content, KNO<sub>3</sub>, KCl, KOH, and others.

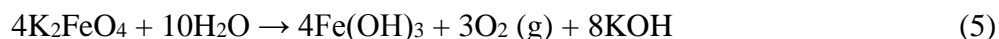
During the purification step, *n*-pentane or benzene was used to replace the moisture content in crude potassium ferrate. Methanol or ethanol was employed to dissolve hydroxides, chlorides, nitrates and other impurities. Diethyl ether could speed up the drying process of crude product. The use of inert solvents to remove moisture from crude products is critical. Otherwise, ferrate will be readily reduced to Fe(OH)<sub>3</sub>, losing its purity grade [21].

For this study, *n*-pentane, rather than benzene, was used due to its lower toxicity and cheaper price. The prices for *n*-pentane and benzene are 80.6 and 96.1 US dollar L<sup>-1</sup>, respectively. The disadvantage of using *n*-pentane is its lower boiling point (36.1 °C) compared to benzene (80.1 °C); this fact implies a greater loss of *n*-pentane if a pilot-scale or full-scale device is to be set up for this purification process, unless it is a closed process. Methanol was chosen, instead of ethanol, because of its cheaper price and greater effectiveness in removing hydroxides, chlorides, nitrates and other impurities [21]. The price ratio of methanol to ethanol is approximately 1/4 and their respective boiling points are 64.7 and 78.4 °C. Diethyl ether will be used to speed up de-moisture rate of crude product.

### 1.4. Stability of Fe(VI)

Fe(VI) is very unstable, readily snatching three electrons from neighboring water and being reduced to a more stable form, Fe(III). Solid-phase hexavalent iron is more stable than aqueous iron. It can be stored with negligible reduction reaction for a long time when it is stored in such a way that keeps off the contact of moisture and atmospheric air [22]. When exposed to moisture and atmosphere, it readily

reacts with water forming  $\text{Fe}(\text{OH})_3$ , oxygen, and potassium hydroxide. The reduction proceeds as follows [22]:



### 1.5. Quantification of Fe(VI)

A few methods can be used for quantitative determination of Fe(VI); they include electrochemical, volumetric, and various spectrophotometric methods [23,24]. Among them, UV-Vis spectral method offers simple steps, rapid experimental work, and accurate outcome [24]. Therefore, this study chooses to use UV-Vis spectral method for determining Fe (VI) concentration and purity. It is briefly described as follows.

Determination of Fe(VI) concentration in water with UV-Vis absorbance is based on Beer's law. Fe(VI) ions in water appears dark purple with an absorbance maximum peak at 505 nm, and its molar absorbance coefficient ( $\epsilon$ ) was determined to be  $1070 \text{ M}^{-1} \text{ cm}^{-1}$  [23]; accordingly, the concentration of Fe(VI) can be calculated using the following equation:

$$\epsilon = A/BC \quad (6)$$

where the notation “ $\epsilon$ ” equals  $1070 \text{ M}^{-1} \text{ cm}^{-1}$  (molar absorbance coefficient), “ $A$ ” is UV-Vis absorbance by sample, “ $B$ ” represents Fe(VI) concentration (M) in the examined sample, and “ $C$ ” is light path (cm) of the quartz cell used in this study.

For determining Fe(VI) purity of the in-house ferrate prepared in the present study, a proper amount of the product was dissolved in 0.100-L de-ionized water, centrifuged for 10 min at 4000 rounds per minute (centrifuge, Allegra 21/R, Beckman Coulter, Brea, CA, USA), and the top clear solution was measured with a UV-Vis spectrometer (UV-2450, Shimadzu Corporation, Tokyo, Japan). In addition, purity of the product in weight percentage can be calculated using the equation below. It has to be noted that molecular weight of  $\text{K}_2\text{FeO}_4$  is  $198.04 \text{ g mole}^{-1}$ :

$$\text{K}_2\text{FeO}_4 \text{ purity} = \frac{A}{1070} \times 0.1 \times \frac{198.04}{\text{weight of sample}} \times 100\% \quad (7)$$

## 2. Materials and Methods

### 2.1. Materials

The spent steel pickling liquid was provided by a local steel plant that uses hydrochloric acid to clean its carbon steel surface. It contains  $133 \text{ g L}^{-1}$  Fe ions and  $351 \text{ g L}^{-1}$   $\text{Cl}^-$ , respectively. The chemicals used in this study are summarized in Table 1.

**Table 1.** Chemicals used in this study.

Chemical	Purity	Producer
Fe(NO <sub>3</sub> ) <sub>3</sub> 9H <sub>2</sub> O	98%–101% (reagent grade)	JT Baker, Center Valley, PA, USA
<i>n</i> -C <sub>5</sub> H <sub>12</sub>	99% (reagent grade)	Merck, Darmstadt, Germany
C <sub>2</sub> H <sub>5</sub> OH	96% (reagent grade)	Merck, Germany.
(C <sub>2</sub> H <sub>5</sub> ) <sub>2</sub> O	99.5% (reagent grade)	Merck, Germany
FeCl <sub>2</sub> 4H <sub>2</sub> O	98% (reagent grade)	Sigma-Aldrich, St. Louis, MO, USA
FeCl <sub>3</sub> 6H <sub>2</sub> O	97% (reagent grade)	Sigma-Aldrich, USA
KOH	85% (reagent grade)	Sigma-Aldrich, USA
NaOH	99% (reagent grade)	Sigma-Aldrich, USA
NaOCl solution	6%–14% (reagent grade)	Sigma-Aldrich, USA
K <sub>2</sub> FeO <sub>4</sub>	purity ≥ 90%	Sigma-Aldrich, USA
MB	100%	Sigma-Aldrich, USA

### 2.2. Synthesis Flowchart for K<sub>2</sub>FeO<sub>4</sub>

Because the spent pickling liquid used here is very rich in Fe and Cl ions, 133 g L<sup>-1</sup> and 351 g L<sup>-1</sup>, respectively, a simple drying process on a 85 °C hot plate can readily vaporize its water content. The solid derived from spent pickling liquid contains FeCl<sub>2</sub> 4H<sub>2</sub>O as the major iron species representing approximately 93%, balanced by 7% FeCl<sub>3</sub> 6H<sub>2</sub>O on mole basis. The iron speciation was determined by Fe *k*-edge X-ray absorption near edge spectrum (XANES) simulation, and the details will be described below in Section 2.4.

K<sub>2</sub>FeO<sub>4</sub> was synthesized using the derived solid as a raw material and the synthesis flowchart is depicted in Figure 1. Briefly, first, 20 g NaOH and 30 mL 6%–14% NaOCl were mixed for one hour at a stirring speed of 800 rpm, and un-dissolved NaOH solid was filtered off and the filtrate was retained and mixed/reacted (stirring at 800 rpm) for 150 min with 2 g of the derived solid. Second, after the centrifuging and solid/liquid separation, liquid solution was mixed with 20 mL saturated KOH, stirred at 800 rpm for 20 min, centrifuged, and solid/liquid separated. The resulting solid material was added into 10 mL 6.0 M KOH. Third, after a centrifuging process at 3500 rpm for 10 min and solid/liquid separation, the liquid portion was added into an icy-cold 20 mL saturated KOH. Finally, this mixture was filtrated and the resulting crude potassium ferrate was subjected to consecutive washing using each of 0.5 mL *n*-pentane, methyl alcohol, and ethyl ether in approximately 2 min. The solid on filter paper was then dried in a vacuum oven (VO-2000, Pan-Chum Co., Taipei, Taiwan) under a pressure < 30 mm Hg at room temperature for one hour to produce dry, purified K<sub>2</sub>FeO<sub>4</sub> product.

### 2.3. Crystalline Phase Study with XRD

X-ray diffractometer (XRD, D8 Advance, Bruker AXS, Karlsruhe, Germany) using a copper target was operated at a voltage of 30 kV and a current of 20 mA. X-ray wavelength generated is 1.54056 Å. Sample scanning angle (2θ) is 20 °–80 ° with a scanning rate of 3 deg min<sup>-1</sup>. Diffraction patterns were identified by comparing them with the database compiled by The Joint Committee on Powder Diffraction Standards (JCPDS).

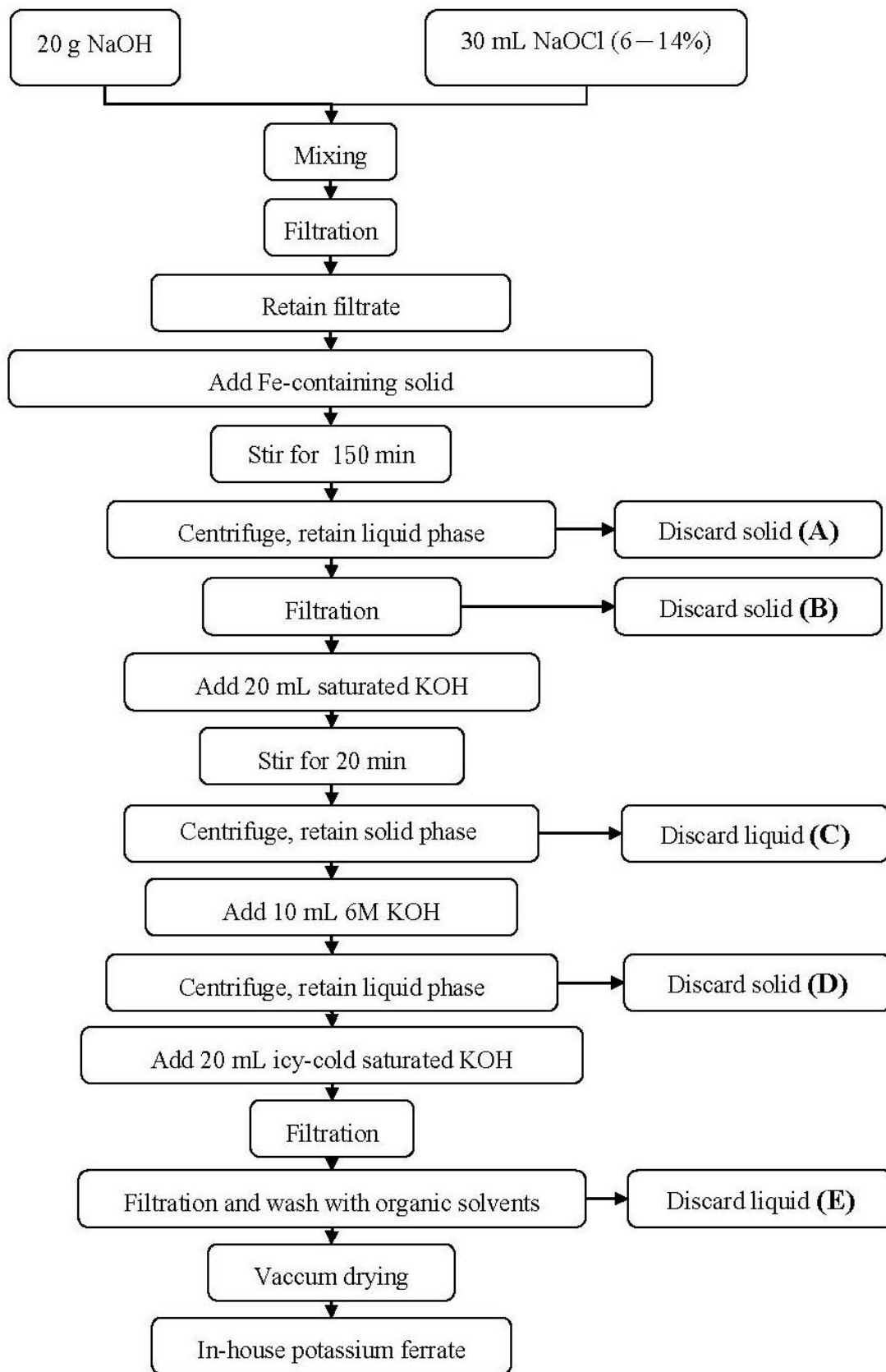


**Figure 1.** Flowchart for synthesizing in-house potassium ferrate.

#### 2.4. Molecular Study of Potassium Ferrates

X-ray absorption spectroscopy is a non-destructive physical method. Generally, an X-ray absorption spectroscopy (XAS) spectrum can be divided into two parts. The first part is X-ray Absorption Near Edge Spectrum (XANES) for probing electronic properties of target atoms, such as oxidation state and electron occupancy of its *d*-orbitals. The second part is Extended X-ray Absorption Fine Structure (EXAFS) that can be Fourier transformed and simulated to reveal the knowledge of local geometry of coordination atoms, such as atomic type, coordination number (*N*), interatomic distance (*R*), and disorder level of coordination atoms ( $\sigma^2$ ).

XAS spectra were recorded on the 16A and Wiggler C (BL-17C) beamlines of National Synchrotron Radiation Center, Hsinchu, Taiwan. During the recording period, its electron storage ring energy was 1.5 GeV, current was 300 mA, and its energy range was 2–14.2 keV. The *k*-edge edge jump of iron is at 7.112 keV. XAS data analysis was carried out using WinXAS 3.1 software [25] (ressler@winxas.de, Thorsten Ressler, Hamburg, Germany). The software can be used to simulate a sample XANES spectrum by linearly combining various standard spectra to quantify component species, based on the least-squares principle from the fingerprints in their XANES spectra [25]. For each standard compound used, two parameters, energy correction and partial mole fraction, are determined. At end of the refining process, standards with a negative mole fraction and/or unreasonable energy shift indicate their absence from the sample [25]. In the present study, XANES spectra from reagent grade FeCl<sub>2</sub> 4H<sub>2</sub>O and FeCl<sub>3</sub> 6H<sub>2</sub>O were recorded and used as standards to simulate the experimental spectrum from dry solid derived from spent pickling liquid.

### 3. Results and Discussion

#### 3.1. Characteristics of Spent Steel Pickling Liquid

##### 3.1.1. pH and Density of Pickling Liquid

Hydrochloric acid was employed by the steel plant for pickling its steel product. The spent pickling liquid has a pH of <1 and a density of 1.40 kg L<sup>-3</sup>. The high density is due to its large contents of Fe and Cl.

##### 3.1.2. Composition of Spent Steel Pickling Liquid

Table 2 shows that the pickling liquid contains many kinds of toxic metals with their concentrations being considerably higher than wastewater legal thresholds. The toxic metals include Cr, Bi, Tl, Cd, Co, Cu, Ni, Pb, and Zn. Fe and Cl are the most abundant components, with Mn and Ca (respectively, 1.386 and 1.551 g L<sup>-1</sup>) being the second most abundant elements. Generally, when Fe content in steel pickling liquid reaches 70–100 g L<sup>-1</sup>, the liquid is disqualified for further pickling process in the steel industry [17]. The spent pickling liquid (Table 2) has apparently been over-used with an Fe content of 133 g L<sup>-1</sup>. Because the sum of Fe and Cl, 485 g L<sup>-1</sup>, accounts for one third of the weight of 1.0 L pickling liquid (*i.e.*, 1.4 kg), only a small amount of heat is required for vaporizing its liquid components, including water and HCl. The pickling liquid was dried on a 85 °C hot plate. Please note that, practically, the HCl can be recovered with a cooling system if desired, but such recovery is not the

objective of the present study, rather, at present we are more focusing on investigating the technical feasibility of using the recovered solid iron chloride(s) as a raw material for preparing potassium ferrate. In contrast, direct use of the pickling liquid in potassium ferrate synthesis would alter the required pH value of the solution containing 20 g NaOH and 30 mL NaOCl, as depicted in Figure 1.

**Table 2.** Chemical compositions of spent steel pickling liquid.

Compositional Element	Content (mg L <sup>-1</sup> )	Spike Recovery <sup>d</sup> (%)
Cr <sup>a</sup>	3.63 ± 0.23	(24 ± 1.2)
Bi <sup>a</sup>	46.48 ± 0.95	(31 ± 4)
Ag <sup>a</sup>	6.86 ± 0.07	(25 ± 3.6)
Al <sup>a</sup>	6.73 ± 0.04	(76 ± 2)
Tl <sup>a</sup>	60.15 ± 0.13	(52 ± 3.1)
Ca <sup>b</sup>	1552 ± 0.3	(97 ± 2.5)
Cd <sup>a</sup>	3.08 ± 0.02	(30 ± 2.4)
Co <sup>a</sup>	5.10 ± 0.036	(31 ± 2.5)
Cu <sup>a</sup>	39.15 ± 0.085	(78 ± 1.4)
Fe <sup>b</sup>	133,000 ± 2160	(89 ± 1.2)
K <sup>a</sup>	7.69 ± 0.00	(111 ± 3.7)
Mg <sup>a</sup>	65.28 ± 0.07	(56 ± 2.6)
Mn <sup>a</sup>	1387 ± 1	(73 ± 0.2)
Na <sup>b</sup>	256.3 ± 1.4	(87 ± 4)
Ni <sup>a</sup>	19.72 ± 0.10	(30 ± 4.1)
Pb <sup>a</sup>	15.08 ± 0.60	(23 ± 2.6)
Zn <sup>b</sup>	188.6 ± 2.1	(91 ± 2.5)
Cl <sup>c</sup>	351,500 ± 3100	(88 ± 3.3)

<sup>a</sup> using an inductively coupled plasma atomic emission spectrometer (ICP-AES, Profile plus, Teledyne Leeman Labs, Hudson, NH, USA) to measure metal concentrations after microwave-assisted digestion;

<sup>b</sup> using a flame atomic absorption spectrophotometer (FAAS, Z-6100, Hitachi, Tokyo, Japan) to measure metal concentrations after microwave-assisted digestion; <sup>c</sup> the total amount Cl ion was measured with an ion chromatographer (IC, DX-100, Dionex, Thermal Fisher Scientific, Sunnyvale, CA, USA); <sup>d</sup> the steps are described as follows. First, the pickling liquid was digested with a microwave digester (MWS-4, Berghof Laborprodukte GmbH, Eningen Germany) at 180 °C; metallic ion concentration in the digest was approximately measured with ICP/atomic emission spectrometer or flame atomic absorption spectrometer. Then, exactly 0.5 to 5 times the amount of the approximate ion concentrations were added to the spent steel pickling liquid and ionic concentrations were re-measured after the same digestion process, providing data for the calculation of spike recovery.

### 3.1.3. Fe Speciation in Solid Raw Material Recycled

As shown in Figure 2, based on XANES simulation, Fe species in the solid raw material recycled by drying the spent steel pickling liquid can be well simulated by approximately summing 93 mol. % ferrous chloride and 7% ferric chloride. The simulative spectrum (dotted curve) and experimental XANES (solid curve) are almost completely overlapped.

As reported in literature, iron sources used in wet oxidation process to synthesize hexavalent iron are mainly ferric chloride and ferric nitrate. Among them, ferric nitrate is preferred due to its characteristics of quick dissolution, rapid chemical reaction with sodium hypochlorite to form



hexavalent iron. Oxidation rate of ferric chloride by sodium hypochlorite is relatively slow because chloride ions released by ferric chloride will slow down the rate of sodium hypochlorite dissociation, thus prolonging Fe(VI) synthesis time [12]. However, ferric chloride costs much less than ferric nitrate. Using reagent grade as an example, price ratio among these iron compounds (per unit iron) is approximately 1.0 (ferric chloride):1.25 (ferrous chloride):2.5 (ferric nitrate). It is noteworthy that reagent grade  $\text{FeCl}_2 \cdot 4\text{H}_2\text{O}$  sells at approximately 120 US dollars  $\text{kg}^{-1}$  in Taiwan.

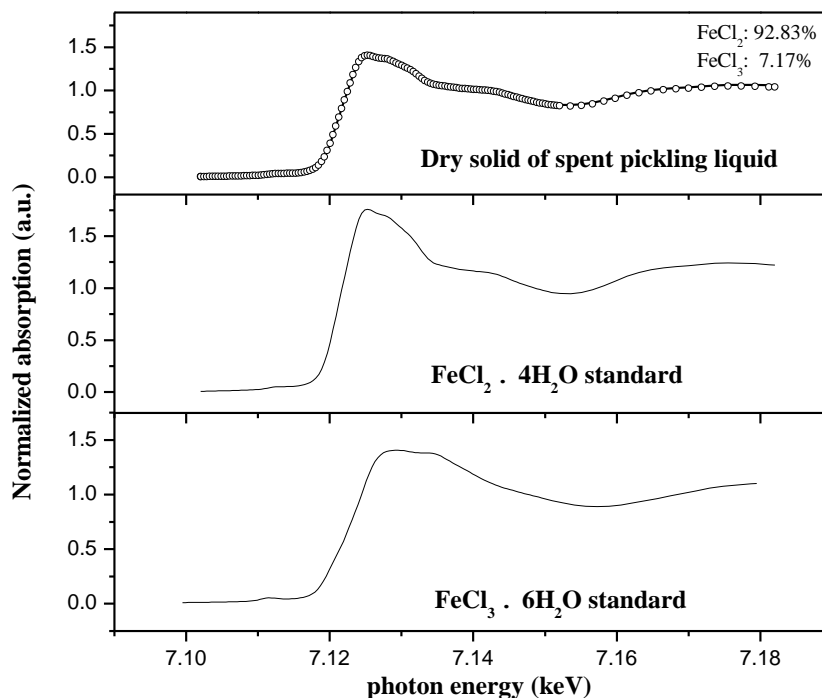


**Figure 2.** XANES simulation-based Fe speciation in solid raw material recycled from spent steel pickling liquid (dotted curve: simulative XANES spectrum being equivalent to 92.83% ferrous chloride plus 7.17% ferric chloride; solid curve: experimental XANES from dry solid of spent steel pickling liquid).

A comparison among various studies in  $\text{K}_2\text{FeO}_4$  synthesis is presented in Table 3. Included in it are types of raw material (iron source), Fe(VI) product purity, and Fe(VI) yield. The yield is calculated based on the following equation.

$$\text{yield (mol. \%)} = \frac{(\text{K}_2\text{FeO}_4 \text{ product weight}) \times (\text{product purity}) \times (\text{Fe atomic weight})}{(\text{K}_2\text{FeO}_4 \text{ molecular weight}) \times (\text{Fe mass in the solid derived from the pickling liquid})} \quad (8)$$

**Table 3.** Purity and yield of potassium ferrate reported in previous studies and this study.

Type of Iron Salt	Oxidizing Agent	Salt Weight (g)	Yield (g)	Purity (wt. %)	Yield (Mol. %)	Literature
$\text{Fe}(\text{NO}_3)_3 \cdot 9\text{H}_2\text{O}$	NaOCl	25	10.43	63.40	53.9	[23]
$\text{FeCl}_3 \cdot 6\text{H}_2\text{O}$	NaOCl	25	9.64	74.71	39.3	[23]
$\text{Fe}(\text{NO}_3)_3 \cdot 9\text{H}_2\text{O}$	NaOCl	- <sup>b</sup>	- <sup>b</sup>	98.5	- <sup>b</sup>	[26]
$\text{Fe}(\text{NO}_3)_3 \cdot 9\text{H}_2\text{O}$	NaOCl	- <sup>b</sup>	- <sup>b</sup>	90	- <sup>b</sup>	[27]
Recycled solid <sup>a</sup>	NaOCl	2	0.254	88	11.7	This study

<sup>a</sup> solid recycled from spent steel pickling liquid; <sup>b</sup> data not reported in both references [25] and [26].

The price of potassium ferrate quite depends on purity. For example, sale price of the Sigma-Aldrich ferrate with  $\geq 90\%$  purity is 99 US dollars  $\text{g}^{-1}$ , while with purity  $\geq 97\%$ , it used to be sold at approximately 350 US dollars  $\text{g}^{-1}$ . Although the yield of our in-house ferrate product is only 12.7%, its purity grade is comparative to the Sigma-Aldrich ferrate with  $\geq 90\%$  purity. It is premature to calculate the cost of our in-house ferrate at present because a pilot-plant scale study is required to make such an estimate. However, for sure, the process reported in the present study can save both raw material costs for ferrous chloride (33 US dollar per mole Fe) and ferric chloride (45 US dollar per mole Fe) and local disposal expense for the spent pickling liquid that is currently about 2500 New Taiwan dollars  $\text{m}^{-3}$  (equivalent to 76.7 US dollars  $\text{m}^{-3}$  based on the exchange rate of 32.6:1 on 3 September 2015). It is noteworthy that local industrial recycling practitioners recover HCl from the spent pickling liquid, but the HCl solution practically recovered contains only 13 wt. % HCl whose industrial application is very limited.

### 3.2. Characteristics of In-House and Commercialized Potassium Ferrates

#### 3.2.1. Chemical Compositions of Potassium Ferrates

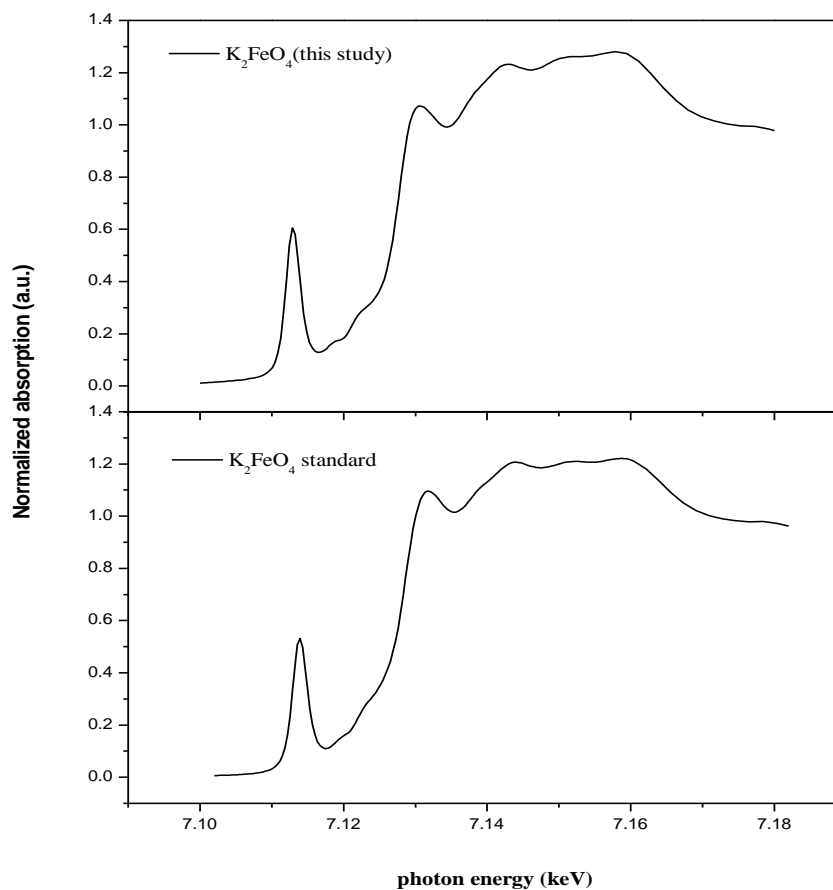
Chemical compositions of the potassium ferrates were analyzed with ICP-AES after their acidic digestion with microwave assistance. Table 4 shows that both in-house and as-purchase Sigma-Aldrich potassium ferrates are of high purity with only negligible impurities. Compared with the commercialized one, the in-house product is no less in purity. Most non-iron metals originally present in the pickling liquid have been either washed or precipitated off during the synthesis process.

Figure 3 depicts Fe *k*-edge XANES spectra from in-house (top) and as-purchase Sigma-Aldrich (bottom) potassium ferrates. The height (or area) of pre-edge peak at 7.115 keV is proportional to the ratio Fe(VI)/total Fe. This figure provides evidence that both ferrates are almost identical in pre-edge peak height, implying that they are of similar purity.

**Table 4.** Chemical compositions of Sigma-Aldrich and in-house potassium ferrates by weight.

Composition	Sigma-Aldrich $\text{K}_2\text{FeO}_4$ Standard		In-House $\text{K}_2\text{FeO}_4$ (This Study)	
	wt. Percentage (%)	Recovery (%)	wt. Percentage (%)	Recovery (%)
Cr <sup>a</sup>	0.11 ± 0	(51 ± 2.5)	0.01 ± 0.0002	(60 ± 2.8)
Bi <sup>a</sup>	0.11 ± 0.0344	(61 ± 1.6)	0.06 ± 0.000196	(51 ± 1.8)
Al <sup>a</sup>	0.01 ± 0.0006	(75 ± 2.6)	0.02 ± 0.00098	(71 ± 2.8)
Ba <sup>a</sup>	0.00 ± 0	(82 ± 2.2)	0.01 ± 0	(88 ± 2.1)
Ca <sup>a</sup>	0.00 ± 0.0004	(73 ± 1.4)	0.02 ± 0.0002	(70 ± 2.6)
Fe <sup>a</sup>	24.99 ± 0.899	(84 ± 2.7)	23.75 ± 0.214	(85 ± 2.1)
K <sup>a</sup>	37.77 ± 0.746	(96 ± 2.5)	38.69 ± 0.697	(94 ± 2.8)
Li <sup>a</sup>	0.20 ± 0.0008	(69 ± 2.3)	0.59 ± 0.00982	(58 ± 1.8)
Mn <sup>a</sup>	0.07 ± 0.002	(80 ± 2.6)	0.10 ± 0.00039	(79 ± 3.1)
Na <sup>a</sup>	0.01 ± 0.0002	(79 ± 1.5)	0.01 ± 0.00039	(77 ± 1.8)
Ni <sup>a</sup>	0.15 ± 0.0656	(69 ± 3.1)	0.04 ± 0.009627	(71 ± 3.0)

<sup>a</sup> analyzed with ICP-AES after microwave-assisted acidic digestion ( $n = 2$ ).



**Figure 3.** Comparison of Fe *k*-edge XANES of in-house  $K_2FeO_4$  and Sigma-Aldrich  $K_2FeO_4$  standard.

### 3.2.2. UV-Vis Absorption Spectra

Previous literature found that hexavalent iron compounds show a maximum absorbance at wavelength 505 nm [3] and two respective minimum absorbance peaks at 390 nm and 675 nm [15] on UV-Vis spectrum. Figure 4 indicates no difference in UV-Vis absorbance spectrum between our in-house potassium ferrate product and the commercial ferrate that was used as a reference compound in this study.

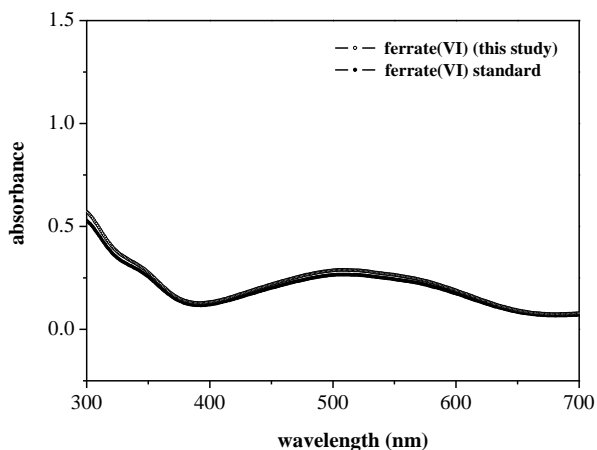


**Figure 4.** UV-Vis absorbance spectra of in-house and Sigma-Aldrich potassium ferrates at a concentration of  $2.88 \times 10^{-4}$  M.

### 3.2.3. SEM-EDX Results from Potassium Ferrates

Figures 5 and 6 depict the mapping results from an environmental scanning electron microscope (ESEM-EDX, FEI Quanta 400 F, Hillsboro, OR, USA) spectra of commercialized and in-house potassium ferrates, respectively. Despite the presence of some impurities, such as Pb, Ca, Si, Al, Mg, Na, and Cl, these two ferrate samples are almost identical in EDX spectrum except that Cl peak of in-house product is slightly stronger. Thus, these two ferrates are considered to be not much different in quality.

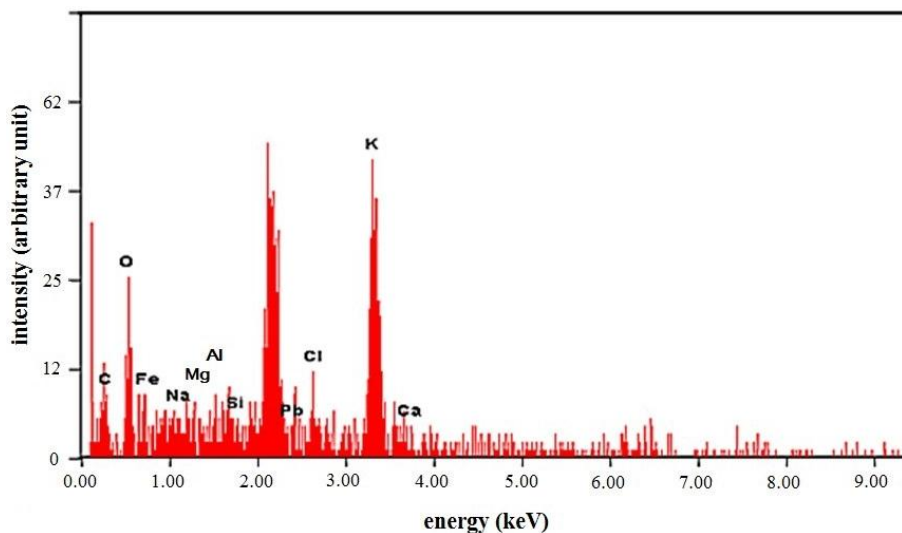


**Figure 5.** SEM/EDX results from as-purchase potassium ferrate.

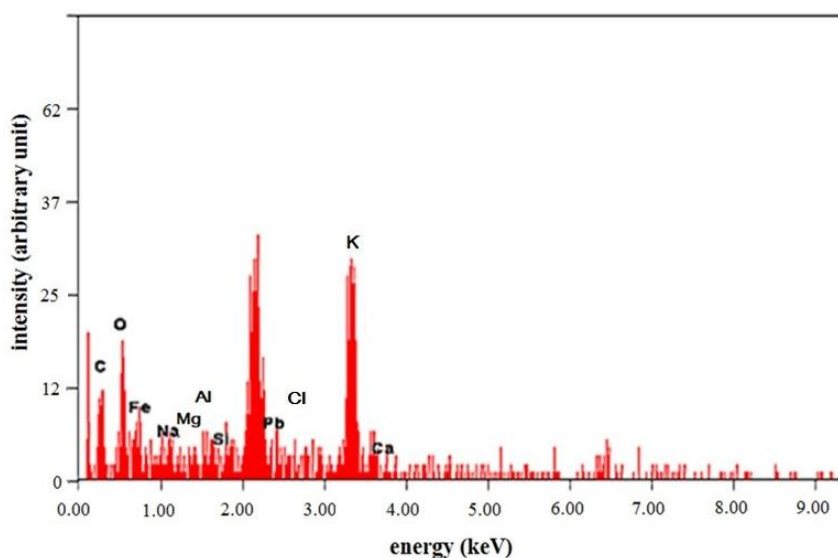


**Figure 6.** SEM/EDX results from in-house potassium ferrate.

### 3.2.4. Crystalline Phases of Potassium Ferrates

Figure 7 indicates that XRD patterns of both in-house and commercialized potassium ferrate are consistent with the main patterns belonging to  $K_2FeO_4$  according to The Joint Committee on Powder Diffraction Standards (JCPDS) 25-0652 data file. XRD patterns also indicate that  $K_2O$  and  $FeO(OH)$  are present as the main impurity in the in-house ferrate product.

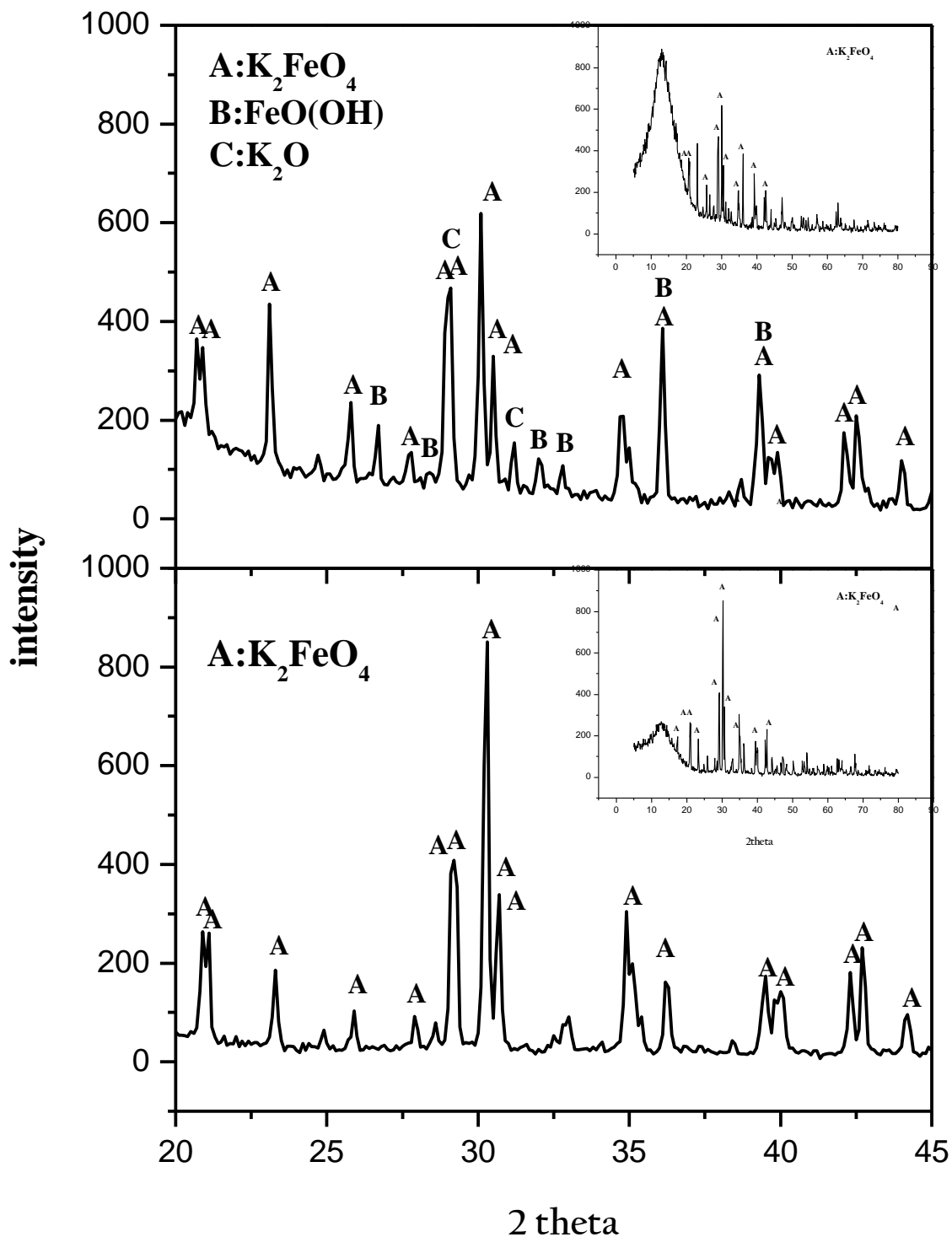


**Figure 7.** XRD patterns of in-house (top) and as-purchase (bottom) potassium ferrates.

### 3.2.5. Test of Fe(VI) Stabilization during Storage

Moisture content was recognized to readily reduce Fe(VI) to Fe(III). Thus dry environment is beneficial for Fe(VI) storage. To test storage stability of in-house Fe(VI) product, two identical parts of it were respectively stored in an electronic dryer box (relative humidity: 35%–40%) and in the atmosphere (relative humidity: 67%–70%) for 32 h, and a small amount of each part was retrieved periodically in every 2–3 h interval for analyzing its Fe(VI) purity. The results are presented in Figure 8.

Figure 8 indicates that for a 32 h storage time, only 1.2% chemical reduction occurred to in-house potassium ferrate when stored under 35%–40% relative humidity (RH), while, if stored under the atmosphere of 67%–70% RH, Fe(VI) reduction rate to Fe(III) was 14.5%. Previous study elsewhere has observed an increase in Fe(VI) reduction with increasing RH at room temperature [28]. At a lower humidity (55%–70% RH), Fe(VI) decay was slow, while the decay rate was considerably enhanced at higher humidity such as 90%–95% RH [28]. Formation of  $\text{KHCO}_3$  at higher RH was suggested to be an important reason for the enhanced Fe(VI) decay rate [28].

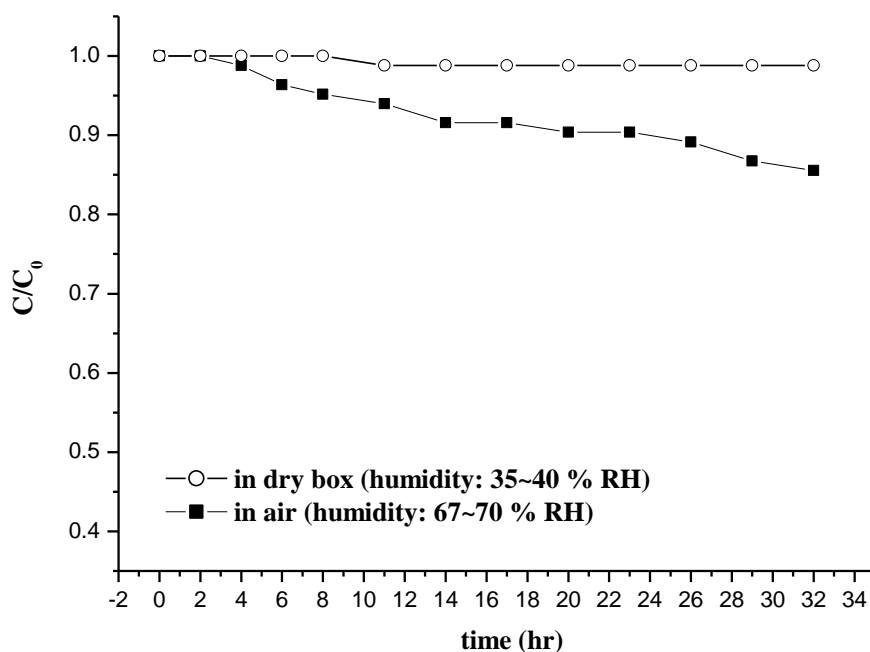


**Figure 8.** Storage stability of in-house potassium ferrate under different relative humidities.

### 3.3. Stepwise Loss of Iron in Fe(VI) Synthesis Flowchart

To know which step(s) have lost a large amount of iron for future studies to improve the yield of in-house potassium ferrate, this study performed quantitative analysis of iron in the solid and liquid phases after each solid/liquid separation step of Fe(VI) synthesis. Fe analysis was carried out with the FAAS after microwave-assisted acidic digestion. Table 5 shows that iron was gradually lost along with the synthesis steps. Among them, the centrifugation and filtration steps affect potassium ferrate yield the most. Ideally, if these iron losses can be reduced, yield of potassium ferrate will be improved.

**Table 5.** Fe loss during wet synthesis of in-house potassium ferrate.

Synthesis Step <sup>b</sup>	Fe Loss <sup>a</sup> (%)
Discarded solid (A)	54.8
Discarded solid (B)	26.5
Discarded liquid (C)	1.49
Discarded solid (D)	8.25
Discarded liquid (E)	0.55

<sup>a</sup> Fe loss =  $\frac{\text{Fe in discarded solid or liquid}}{\text{total Fe used for synthesis}}$ ; <sup>b</sup> please refer to Figure 1.

### 3.4. MB De-Colorization with In-House Potassium Ferrate

To verify how the in-house potassium ferrate performed in treating pollutants, it was employed to de-colorize aqueous MB, a frequently used dye in dyeing sector. For the de-colorization test, two Fe/C mole ratios, 2/1 and 1/1, were used, given that the oxidation state of carbon of MB molecules will generally be increased from 0 to 4+ while Fe(VI) will be reduced to Fe(III) by a decrease of 3+ oxidation state. Figure 9 depicts time-dependence of methylene blue de-colorization with in-house potassium ferrate, and within 30 min, all MB molecules are de-colorized at a Fe/carbon ratio of 2/1. This fact proves the effectiveness of the in-house product.

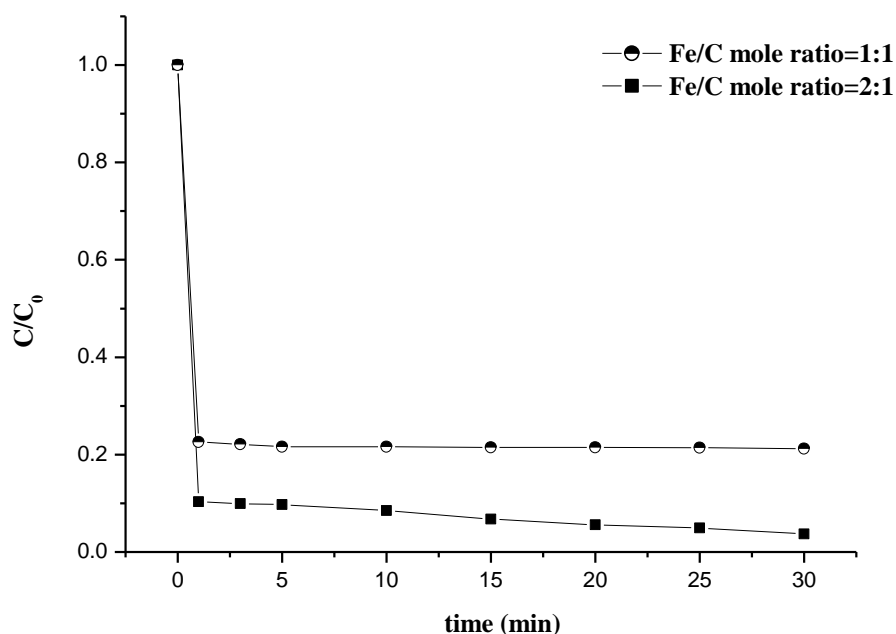


**Figure 9.** Time-dependence of methylene blue de-colorization by in-house potassium ferrate at two Fe/C mole ratios.

## 4. Conclusions

A spent hazardous steel pickling liquid was recycled as iron chlorides for synthesizing high-purity in-house potassium ferrate. Below are the conclusions.

First, the spent steel pickling liquid is very rich in iron and chloride ions, being co-existent with various toxic metals that makes the pickling liquid hazardous. Despite the hazardous nature of pickling liquid, after drying as solid material, it was successfully used as a raw material for synthesizing  $K_2FeO_4$ . The derived solid material mainly consists of 7% ferric chloride and 93% ferrous chloride, as revealed by Fe *k*-edge XANES simulation.

Second, as supported by the characterization results from using instruments including SEM-EDX, UV-Vis absorbance spectroscopy, XRD, and XAS, the in-house potassium ferrate product is not inferior to the commercialized ferrate. Varieties of impurity present in the spent steel pickling liquid do not affect the purity of in-house potassium ferrate, compared with the commercialized one.

Third, for a 32 h storage time, only 1.2% decay occurred to in-house potassium ferrate when stored under 35%–40% RH. If stored in an electronic dryer box to effectively cut off contact of atmospheric

air, the in-house potassium ferrate can seemingly remain stable without being chemically reduced for a period of time longer than 32 h.

Fourth, the test of methylene blue de-colorization confirms that the in-house potassium ferrate has great oxidation capability to break down pollutants in water.

Finally, for future study, industrial grade chemicals will be used to replace the reagent-grade chemicals for the synthesis of in-house potassium ferrate.

### Acknowledgments

This work was sponsored by the Taiwan Ministry of Science and Technology (NSC- 102-2221-E-029-001). Fe *k*-edge XAS was recorded on beamlines 17C and 16A of NSRRC, Taiwan.

### Author Contributions

Wang and Liu worked together in laboratory under Wei's advice for the project. They also did some literature review. Wei was the principal investigator of the project sponsored by the Taiwan Ministry of Science and Technology and this paper was written by Wei after discussion with Wang and Liu.

### Conflicts of Interest

The authors declare no conflict of interest.

### References

1. Audette, R.J.; Quail, J.W.; Smith, P.J. Ferrate(VI) ion, a novel oxidizing agent. *Tetrahedron Lett.* **1971**, *3*, 279–282.
2. Yoon, J.; Lee, Y.; Cho, M.; Kim, J.Y. Chemistry of ferrate (Fe(IV)) in aqueous solution and its application as a green chemistry. *J. Ind. Eng. Chem.* **2004**, *10*, 161–171.
3. Jiang, J.Q.; Lloyd, B. Progress in the development and use of ferrate(VI) salt as an oxidant and coagulant for water and wastewater treatment. *Water Res.* **2002**, *36*, 1397–1408.
4. Jiang, J.Q. The role of ferrate(VI) in the remediation of emerging micro pollutants: A review. *Desalin. Water Treat.* **2015**, *55*, 828–835.
5. Sharma, V.K.; Zboril, R.; Varma, R.S. Ferrates: Greener Oxidants with Multimodal Action in Water Treatment Technologies. *Acc. Chem. Res.* **2015**, *48*, 182–191.
6. Kim, C.; Panditi, V.R.; Gardinali, P.R.; Varma, R.S.; Kim H.; Sharma, V.K. Ferrate promoted oxidative cleavage of sulfonamides: Kinetics and product formation under acidic conditions. *Chem. Eng. J.* **2015**, *279*, 307–316.
7. Yates, B.J.; Zboril, R.; Sharma, V.K. Engineering aspects of ferrate in water and wastewater treatment—A review. *J. Environ. Sci. Heal. A.* **2014**, *49*, 1603–1614.
8. Gombos, E. Ferrate treatment for inactivation of bacterial community in municipal secondary effluent. *Bioresour. Technol.* **2012**, *107*, 116–121.



9. Prucek, R.; Tucek, J.; Kolarík, J.; Hušková, I.; Filip, J.; Varma, R.S.; Sharma, V.K.; Zboril, R. Ferrate(VI)-Prompted removal of metals in aqueous media: Mechanistic delineation of enhanced efficiency via metal entrenchment in magnetic oxides. *Environ. Sci. Technol.* **2015**, *49*, 2319–2327.
10. Gombos, E.; Barkacs, K.; Felföldi, T.; Vertes, C.; Mako, M.; Palko, G.; Zárny, G. Removal of organic matters in wastewater treatment by ferrate(VI) technology. *Microchem. J.* **2013**, *107*, 115–120.
11. Sharma, V.K. Oxidation of inorganic contaminants by ferrates (VI, V, and IV) kinetics and mechanisms: A review. *J. Environ. Manag.* **2011**, *92*, 1051–1073.
12. Jiang, J.Q.; Lloyd, B. Preliminary study of ciprofloxacin (cip) removal by potassium ferrate(VI). *Sep. Purif. Technol.* **2013**, *88*, 95–98.
13. Li, C.; Lib, X.Z.; Graham, N.; Gao, N.Y. The aqueous degradation of bisphenol A and steroid estrogens by ferrate. *Water Res.* **2008**, *42*, 109–120.
14. Yang, X.; Guo, W.; Zhang, X.; Chen, F.; Wei, T. Formation of disinfection by-products after pre-oxidation with chlorine dioxide or ferrate. *Water Res.* **2013**, *47*, 5856–5864.
15. Al-Abdulya, A.; Sharma, V.K. Oxidation of benzothiophene, dibenzothiophene, and methyl-dibenzothiophene by ferrate(VI). *J. Hazard. Mater.* **2015**, *279*, 296–301.
16. Environmental Protection Administration, R.O.C. Available online: <http://www.epa.gov.tw/> (accessed on 21 September 2015).
17. Agrawal, A.; Sahu, K.K. An overview of the recovery of acid from spent acidic solutions from steel and electroplating industries. *J. Hazard. Mater.* **2009**, *171*, 61–75.
18. Rögener, F.; Buchloh, D.; Reichardt, T.; Schmidt, J.; Knaup, F. Total regeneration of mixed pickling acids from stainless steel production. *Stahl und Eisen.* **2009**, *10*, 69–73.
19. Perfiliev, Y.D.; Benko, E.M.; Pankratov, D.A.; Sharma, V.K.; Dedushenko, S.K. Formation of iron(VI) in ozonolysis of iron(III) in alkaline solution. *Inorg. Chim. Acta* **2007**, *360*, 2789–2791.
20. Thompson, J.E.; Ockerman, L.T.; Schreyer, J.M. Preparation and purification of potassium ferrate(VI). *J. Am. Chem. Soc.* **1951**, *73*, 1379–1381.
21. Delaude, L.; Laszlo, P. A Novel Oxidizing Reagent Based on Potassium Ferrate(VI). *J. Org. Chem.* **1996**, *61*, 6360–6370.
22. Sharma, V.K. Potassium ferrate(VI): An environmentally friendly oxidant. *Adv. Environ. Res.* **2002**, *6*, 143–156.
23. Licht, S.; Naschitz, V.; Halperin, L.; Halperin, N.; Lin, L.; Chen, J.J.; Ghosh, S.; Liu, B. Analysis of ferrate(VI) compounds and super-iron Fe(VI) battery cathodes: FTIR, ICP, titrimetric, XRD, UV-VIS, and electrochemical characterization. *J. Power Sources* **2001**, *101*, 167–176.
24. Luo, Z.; Strouse, M.; Jiang, J.Q.; Sharma, V.K. Methodologies for the analytical determination of ferrate(VI): A Review. *J. Environ. Sci. Heal. A* **2011**, *46*, 453–460.
25. Ressler, T. WinXAS: A program for X-ray absorption spectroscopy data analysis under MS-Windows. *J. Synchrotron Radiat.* **1998**, *5*, 118–122.
26. Wang, L.W.; Liu, S.Q.; Zhang, X.Y. Preparation and application of sustained release microcapsules of potassium ferrate(VI) for dinitro butyl phenol (DNBP) wastewater treatment. *J. Hazard. Mater.* **2009**, *169*, 448–453.
27. Yuan, B.L.; Li, X.Z.; Graham, N. Reaction pathways of dimethyl phthalate degradation in TiO<sub>2</sub>-UV-O<sub>2</sub> and TiO<sub>2</sub>-UV-Fe(VI) systems. *Chemosphere* **2008**, *72*, 197–204.

28. Machala, L.; Zboril, R.; Sharma, V.K.; Filip, J.; Jancil, D.; Homonnay, Z. Transformation of solid potassium ferrate(VI) ( $K_2FeO_4$ ): Mechanism and kinetic effect of air humidity. *Eur. J. Inorg. Chem.* **2009**, *8*, 1060–1067.

© 2015 by the authors; licensee MDPI, Basel, Switzerland. This article is an open access article distributed under the terms and conditions of the Creative Commons Attribution license (<http://creativecommons.org/licenses/by/4.0/>).